Journal of Computers Vol. 35 No. 4, August 2024, pp. 175-190
doi: 10.53106/199115992024083504013

Design and Path Planning Method of Control System for Photovoltaic Panel Cleaning Robot

Li-Wei Jin[1], Guang-Shuang Meng[2*], Hong-Liang Zheng[1], Jing Zhang[1], Shi-Hui Dong[1], Xue Deng[3], and Zhi-Yuan Zhang[4]

[1] School of Automation Engineering, Tangshan Polytechnic University, Tangshan City 063299, Hebei Province, China
{liwei89786, mgs97987, hongliang8834, jingjing567, hui8978}@126.com

[2] Bingtuan Xingxin Vocational and Technical College, Tiemenguan City 841007, Xinjiang Uygur Autonomous Region, China
[3] Tangshan Urban Drainage Co., Ltd, Tangshan City 063000, Hebei Province, China
98798748@qq.com

[4] School of Electronic and Information Engineering, Beijing Jiaotong University, Beijing 100044, China
zhangzhiyuan@bjtu.edu.com

Received 19 July 2024; Revised 31 July 2024; Accepted 15 August 2024

Abstract. As the proportion of photovoltaic power generation continues to increase, the number of photovoltaic panels installed is also increasing. In response to the direct impact of dust and sand blocking the surface of photovoltaic panels on power generation efficiency, as well as the high cost and low efficiency of daily manual maintenance, this paper designs a photovoltaic panel surface cleaning robot and elaborates on the main structure of the robot: cleaning module and moving module. In order to enable the robot to efficiently complete cleaning work, the robot's movement trajectory on the photovoltaic surface is planned. The planning method adopts a control strategy combining neural network and PID. Then, the machine's control system is designed based on the planning method. Finally, through experimental verification, the rationality of the robot's cleaning structure design is analyzed and verified, and the cleaning efficiency of the robot is improved.

Keywords: photovoltaics, robot, path planning, PID

1 Introduction

Photovoltaic power generation has attracted attention from various countries due to its lower maintenance costs and lower power generation costs, as its widespread application is mainly in remote areas with sufficient sunlight and fewer buildings, without occupying densely populated areas. According to the statistics of the International Energy Agency, the global increase in photovoltaic power generation will reach 110-120GW by 2022, and China's new installed capacity will reach 60GW by 2023. So solar photovoltaic power generation, as a new type of renewable energy, has become an important way for people to obtain electricity in their daily lives [1].

In the photovoltaic power generation system, the photovoltaic panel is the main equipment for power generation. The principle of power generation is that the photovoltaic panel generates a voltage difference through the flow of electrons between two layers of semiconductors under the action of light, thereby realizing the conversion of light energy into electrical energy. Therefore, increasing the duration and amount of light exposure, as well as improving the efficiency of converting light energy into electrical energy, can increase the power generation of photovoltaic panels. In order to obtain sufficient light intensity and duration, most large photovoltaic power plants choose to be built in the northwest region where precipitation is low, air humidity is low, and light is relatively sufficient, but the air is filled with a large amount of dust particles, which is an area with poor human living conditions. With the continuous development of the photovoltaic industry, in order to improve the utilization of urban space, rooftop photovoltaic power stations are also being vigorously constructed and put into

* Corresponding Author

use, especially in the flat roofs of rural areas in the north, where the investment of rooftop photovoltaics can be seen everywhere. Whether in the northwest region or on human rooftops, the main factor affecting the power generation efficiency of photovoltaic panels is the accumulation of dust, which leads to the shading of the panels. Therefore, the most important way to improve the electrical efficiency of photovoltaic panels is to regularly clean and remove dust from the surface of the panels. Research has shown that the power generation efficiency of photovoltaic panels can be reduced by up to 40% due to dust cover [2].

Summarizing the existing cleaning methods for photovoltaic panels, there are mainly the following:

1) Manual cleaning: refers to the complete use of human labor to clean the surface of photovoltaic panels. For small photovoltaic power plants, manual cleaning is relatively flexible and convenient. However, for large photovoltaic power plants, manual cleaning incurs high costs in terms of manpower, water sources, and other aspects, which actually increases the daily operation and maintenance costs of the photovoltaic power plant [3].

2) Photovoltaic cleaning vehicle: Professional cleaning tools such as cleaning brushes and flushing nozzles are installed on photovoltaic cleaning vehicles, which are operated and cleaned by professional operators. The use of photovoltaic cleaning vehicles has a significant effect on reducing labor costs, but the cleaning vehicle body is relatively large, requiring high requirements for the overall layout of photovoltaic power station panels, as well as the spacing and terrain between panels [4].

3) Orbital cleaning robot: This type of robot is installed on the photovoltaic panel track, and during operation, the robot runs along the track with the plane coordinate axis as the reference for operation. The installation cost of robots is relatively high, so they are only suitable for large-scale centralized photovoltaic power plants. Traditional rail robots lack corresponding monitoring methods and cannot receive timely handling when faults occur.

4) Portable photovoltaic cleaning robot: a small photovoltaic cleaning robot, similar to a sweeping robot, equipped with more professional photovoltaic cleaning tools. Portable photovoltaic cleaning robots are lightweight and compact, mostly used for cleaning distributed photovoltaic panels [5].

In summary, there are still many shortcomings in the current cleaning methods for large-scale centralized photovoltaic panel arrays. For this purpose, this article has designed an intelligent photovoltaic cleaning robot that can achieve intelligent cleaning work, while also having remote monitoring, fault alarm and other functions. The overall function runs smoothly, comprehensively improving the cleaning effect and efficiency of photovoltaic panels.

The research object of this article is a large photovoltaic power station, where the photovoltaic panel array has a large area and wide distribution. It is difficult to complete the cleaning work of the photovoltaic panel once, and manual wiping and rinsing with clean water are mainly used. The cleaning effect is poor and requires a lot of time to complete. Subsequently, specialized cleaning robots for photovoltaics emerged, which can overcome the drawbacks of expensive and time-consuming manual cleaning. Generally, cleaning robots for panel operations are divided into two types: track type and mobile type. Track type robots install guide rails on photovoltaic panels and drive up and down cleaning brushes to clean the entire photovoltaic panel by moving them in plane coordinates. The objects cleaned by orbital robots are generally single row panels, while mobile robots have low cleaning efficiency and require multiple mobile cleaning robots for use in large power plants, resulting in high costs. Therefore, existing cleaning robots mainly use orbital photovoltaic cleaning robots to clean the surface of photovoltaic panels through timed and short cycle cleaning.

Analyzing the current usage status of photovoltaic panel robots, this article aims to meet the practical needs of panel cleaning and designs an autonomous mobile robot that utilizes a wheeled structure for autonomous navigation and movement. It is suitable for various scales of photovoltaic arrays and has higher robot usage efficiency. For photovoltaic power plants, there is no need to adjust the layout of photovoltaic panels, and the customized robot function scheme is more in line with the concepts of universality and economy in this article.

This article focuses on the autonomous mobile photovoltaic cleaning robot to complete the following tasks:

1) Designed and completed the overall structure of the robot, and designed each component of the robot. Optimized the design of the core structure - cleaning mechanism. Then, in order to analyze the fatigue strength of the cleaning mechanism, finite element modeling and analysis were carried out to verify its working strength and improve the structural design;

2) The control system scheme design for the mobile robot has been completed. This paper adopts PID control strategy. For the important parameter settings in the control strategy, BP neural network algorithm is used for optimization. The parameter results obtained can make the PID control strategy reach the optimal level.

3) Using the existing layout of photovoltaic panels as a structured environment, path planning is carried out for the robot to ensure that the robot's motion trajectory can better fit the predetermined trajectory.

4) Build a simulation environment to conduct simulation experiments on the robot's motion trajectory, and calculate the deviation between the actual motion trajectory and the real trajectory.

2 Related Work

In terms of structural design of photovoltaic cleaning robots, there are several typical representatives: Ecoppia E4 robot, Washpanel, NOMAD robot.

Ecoppia E4 is a non fully autonomous orbital photovoltaic panel cleaning robot, whose cleaning structure mainly consists of cleaning brushes. In the selection process of cleaning brushes, softer materials were chosen, resulting in weaker mud and dirt removal ability of the cleaning brushes. Therefore, it is more suitable for cleaning surface dust in single row panels in dry and sandy environments. Ecoppia E4 requires manual installation of rails to secure the robot before use, and the robot moves horizontally and vertically through the rails.

The Washpanel cleaning robot comes from Italy and works by horizontally moving the cleaning structure on the photovoltaic panel to clean it. In terms of the design of the cleaning structure, the length range of the cleaning brush selected is 1-16 meters. At the same time, the robot cleaning structure includes a water pipe interface. During the cleaning process, clean water can be used to wet the dirt on the panel, reducing the adhesion of the dirt on the panel [6].

The NOMAD cleaning system has a similar cleaning structure to the Ecoppia E4 robot, and is an waterless cleaning structure, so its working environment is also in desert and other sand and dust scenes. In addition to not using water during the cleaning process, NOMAD robots also have some advanced control functions, such as self starting cleaning and remote control, which are more complete. Therefore, compared to Ecoppia E4 robots, NOMAD robots have a higher market share. In terms of cleaning efficiency, NOMAD robots can clean about 1680 m^2 photovoltaic panels per hour [7].

In the design of robot control systems, there are two typical control theories: layered control and PID control. Hierarchical control is a hierarchical control concept that establishes an objective function through tracking performance and driving performance during the tracking control process, designs an optimal controller, and then designs a low-speed tracking controller based on the results of the optimal controller to track the target speed. And this article takes PID control theory as the control basis, so the existing applications of PID control theory are summarized as follows:

Jishuang Xu from Anhui Agricultural University mainly focuses on transportation robots and studies path planning and autonomous navigation problems during transportation. His robot's application scenario is in poultry and livestock landfill sites, which are typical structured environments. Therefore, he proposes a transportation robot path planning method based on the improved $A\sim^{*}$ algorithm and a motion control method based on PID theory. Then, the Manhattan distance algorithm is used to calculate the distance from the endpoint to the starting point, and the heuristic function is improved using added values and weights to improve the path planning algorithm. Finally, the Bessel curve function is introduced to optimize the path, and the PID algorithm based on fuzzy theory is used to control the linear velocity and angular velocity of the transportation robot chassis to track and walk the planned path. The results show that the deviation between the PID control path and the planned path is within a reasonable range [8].

Lin Peng from Nanhua University proposed a robot yaw angle control strategy based on PID control theory to improve the driving stability of small wheeled robots and reduce automatic driving errors. Firstly, the dynamic characteristic model of the robot's automatic driving system and the simulation model based on fractional order PID yaw angle control system were analyzed and constructed. In order to verify the precision of control theory, MATLAB/Simulink software was used to track and simulate the motion process of the robot. The response curves of the robot's motion speed, angular acceleration, displacement, etc. within 10 meters were obtained, and compared with the response curves of the robot performing the same motion under the improved PID control strategy. The results showed that compared with traditional PID control, the robot using fractional order PID control strategy automatically reduced the center of mass lateral angle by 71.4%, the lateral angular velocity by 23.6%, and the lateral offset by 29.5% within a motion distance of 10 meters. The control results met the experimental requirements [9].

In terms of robot path planning, the grid map based path planning method is suitable for path planning based on photovoltaic panel array scenes. The core idea of this method is to divide the map into regular unit grids and then use algorithms to find the optimal method that covers all grids.

Zhengfeng Liu, the research object is the impact of map grid segmentation on path planning in actual environments, and explores the application of Algorithm A^* in grid map path planning. In practical analysis, taking the domestic marine environment as an example, a comparative analysis of path planning was conducted on grid maps at different scales. After experiments, it was found that grid mapping of environmental maps significantly improves the efficiency of path planning. Reasonably adjusting the equivalent grid settings at obstacle boundaries can ensure the connectivity of path planning space and improve the efficiency and success rate of path planning [10].

Keyin Wang, in order to solve the problems of slow convergence speed, multiple iterations, and unstable convergence results when applying traditional reinforcement learning algorithms to path planning in unknown environments of mobile robots, used Q-learning algorithm and proposed improvement strategies for the algorithm based on practical problems. Introducing the artificial potential field method during state initialization, based on the theory of artificial potential field, the endpoint potential field is minimized, guiding the intelligent agent to approach the minimum point of the potential field infinitely, reducing the ineffective probing caused by environmental exploration in the initial stage of the algorithm. When the intelligent agent approaches the most important point, the improved ε greedy strategy is used to adjust the robot pose. By dynamically adjusting the greedy factor ε, it can help the robot balance the relationship between exploration and utilization, accelerate the convergence speed of the algorithm, and improve the stability of the convergence results. Therefore, the control idea in this paper can be used as a reference [11].

In summary of the above research results, this article aims to complete the system design and path planning of robots. The overall structure of the article consists of the following parts:

The second chapter mainly lists the relevant research results and references existing control strategies. The third chapter mainly introduces the structural design process of the robot and the detailed functional design of each part. The fourth chapter mainly completes the design of the control system and the path planning method of the robot. Chapter 5 is the simulation experiment process of robot path planning and the analysis of the experimental results. Chapter 6 is the conclusion section, which summarizes this article and analyzes its shortcomings, while also providing prospects for future research directions.

3 Structural Design of Photovoltaic Robots

Based on the current usage of photovoltaic power stations, due to the complex geographical environment and different installation methods of photovoltaic panels, the installation of photovoltaic modules is also relatively complex. To summarize the characteristics of different application scenarios, this article summarizes the functional design parameters of photovoltaic cleaning robots from the perspective of mechanical design as follows:

(1) In Chinese Mainland, large photovoltaic power stations are generally built in high latitude areas with rich solar energy resources and less rainfall, such as the desert areas in northwest China, where the climate is dry and the wind and sand are heavy. In order to save water resources, robots are generally required to use the method of anhydrous dedusting, but the cleaning effect of the anhydrous mode is poor. Therefore, this paper designs the robot as a switchable function of anhydrous and water mode, so that the robot can adapt to different working environments [12].

(2) In order to obtain more solar energy resources, photovoltaic modules are usually installed in a tilted fixed manner, and the installation angle is related to factors such as local latitude and lighting angle. Generally, the tilt angle is in the range of 30 ° to 60 °. Therefore, it is required that the robot can move horizontally and vertically on the inclined surface of the photovoltaic module array, and the robot will not detach or experience idling from the surface of the photovoltaic module.

(3) Considering that the gravity of the robot itself will generate significant mechanical pressure on the surface of the photovoltaic panel, the overall design of the robot requires a simple and reasonable mechanical structure. When selecting materials, materials with low density, high strength and stiffness, and good economy should be chosen to reduce material costs while reducing the overall weight of the robot, ensuring that the robot will not cause damage to the photovoltaic modules due to its own weight during operation.

(4) For the convenience of later maintenance and upkeep of robots, standard parts are selected as much as possible during robot design. When robot components are damaged or severely worn, they can be replaced at any time to reduce the cost of later operation and maintenance of robots.

(5) The installation of photovoltaic modules is affected by terrain and in order to reduce obstruction between

various photovoltaic panels, there is a height difference between photovoltaic modules. In order to ensure that robots can smoothly pass through the intersection of photovoltaic arrays, connecting beams are often used to connect photovoltaic arrays. The height difference between adjacent photovoltaic modules causes a certain slope in the connecting beams, so robots need to have a certain ability to overcome obstacles and climb slopes.

(6) When the robot is working, it will block the photovoltaic modules, affecting the power generation efficiency of the photovoltaic modules, and staying on the surface of the photovoltaic modules for a long time will cause local overheating. When the temperature is too high, the photovoltaic modules will be burned. Therefore, a parking rack needs to be designed at the end of the photovoltaic array. After the robot completes the cleaning, it will automatically return to the parking rack and wait for new operation instructions [13].

The overall framework of the photovoltaic panel cleaning robot is shown in Fig. 1.

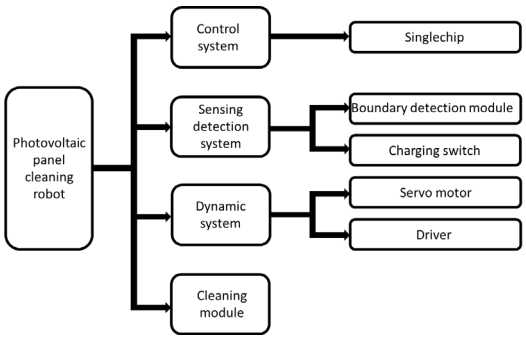

Fig. 1. Overall structural design of robots

The design of the robot was carried out using SolidWorks software. After design, the structure of the robot is shown in Fig. 2.

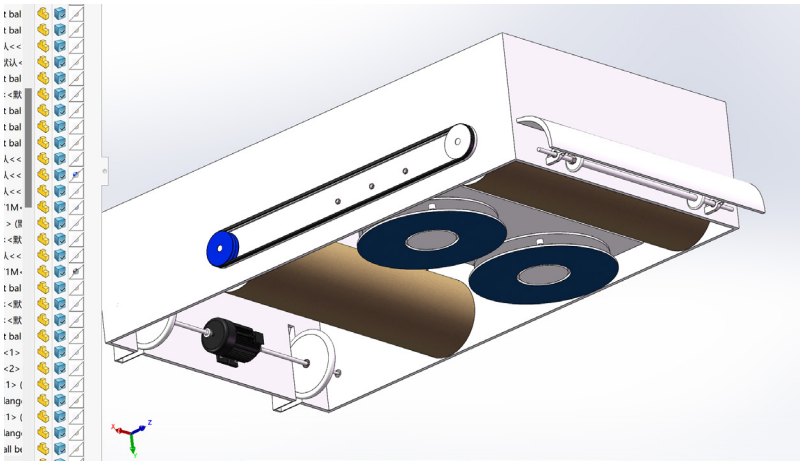

Fig. 2. Three dimensional structure of robots

3.1 Selection of Servo Motors

The weight of the robot is based on the model designed by SolidWorks. As the photovoltaic panel remains tilted, the force acting on the robot during movement is shown in Fig. 3.

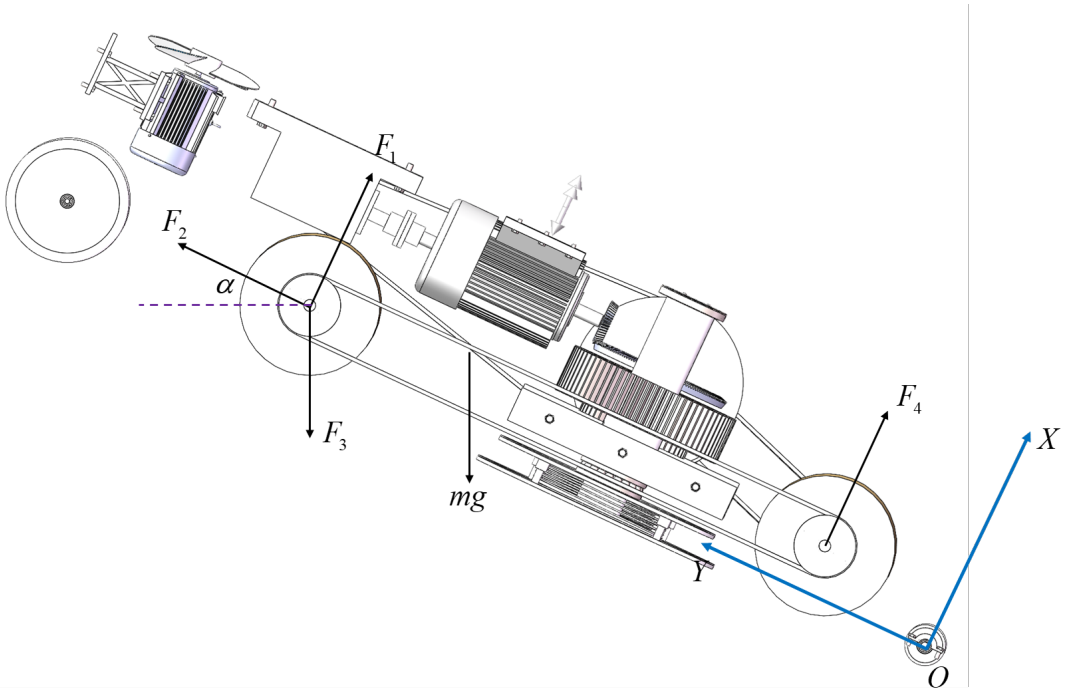

Fig. 3. Force analysis

In Fig. 3, point O is the origin of the spatial coordinate system. The normal direction of the photovoltaic module surface is the forward direction of the x -axis, and the upward direction along the photovoltaic module surface is the forward direction of the y -axis. The spatial coordinate system is established according to the right-hand rule [14]. The robot as a whole needs to meet the static balance and torque balance, so the static equation of the robot is:

$$\begin{cases} F_2 = mg\sin\alpha \\ F_3 = 2F_s / \sqrt{15} \\ F_1 + F_4 - F_3 = mg\cos\alpha \\ F_4 y_{AB} - mg\cos\alpha \cdot y_{AC} - mg\sin\alpha \cdot x_{AC} = 0 \end{cases} \tag{1}$$

In the formula: A represents the mass of the robot, and F_i= (i = 1, 2, 3, 4) represents the support force of the photovoltaic module on the robot's contact point; α is the installation angle of the photovoltaic module; y_{AB} , y_{AC}, x_{AC}, y_{BC} are the projected lengths between the subscript points on the y -axis and x -axis; F_s is the tension force.

The support force F1 of the photovoltaic module for the robot is the contact pressure between the robot's track walking part and the photovoltaic module, so the required driving force for the robot is:

$$F_T = f_1 F_1. \tag{2}$$

F_T is the required driving force for the robot (ignoring the friction between the rolling brush and the surface of the photovoltaic module); f_1 is the rolling friction coefficient between the rubber wheel and the surface of the photovoltaic module. By using SolidWorks software, the mass m of the robot is estimated to be 20kg, the installation angle α of the photovoltaic module is 45°, the rolling friction coefficient f_1 on the surface of the rubber wheel and photovoltaic module is 0.3, the pre tension force F_s of the tension spring in the rear tensioning mechanism is 100N, and the radius R of the active belt wheel wrapping the track is 55mm, y_{AB} , y_{AC}, x_{AC}, y_{BC} which are 572mm, 87mm, 61.3mm, and 496mm, respectively. Based on the above analysis, the output torque of the robot's walking drive motor should be greater than 3.64 $N{\cdot}m$.

The minimum driving power P_1 of the walking drive motor is:

$$P_1 = \frac{2\pi nM}{60}. \tag{3}$$

If the walking speed of the robot is set to 12-20 *m*/min, the rotational speed *n* can be obtained through the wheel diameter. Based on the above analysis, the minimum driving power P_1 of the walking drive motor is calculated to be 22.06*W*. Therefore, a DC motor model 40W-24GN-30S was selected and equipped with a planetary reducer (4GN50K) with a reduction ratio of 50. The performance parameters and external dimensions of the motor are shown in Table 1.

Table 1. List of DC motor parameters

Parameter	Parameter values
Rated Power	40W
Rated Voltage	24V
Output Speed	60RPM
Output Torque	4.82 $N \cdot m$
Number of Teeth	40
Winding Inductance	4.2 mH
Phase Current	2 A
Moment of Inertia	0.48 $kg \cdot cm^2$
Viscous Damping	0.07

3.2 Cleaning Device Design

The robot has functions such as walking, switching between water and water cleaning modes, comprehensive coverage cleaning, intelligent start stop, etc. It can intelligently clean the external environment's light changes and boundary distances. The mechanical structure of the photovoltaic panel cleaning robot designed in this article is shown in Fig. 4.

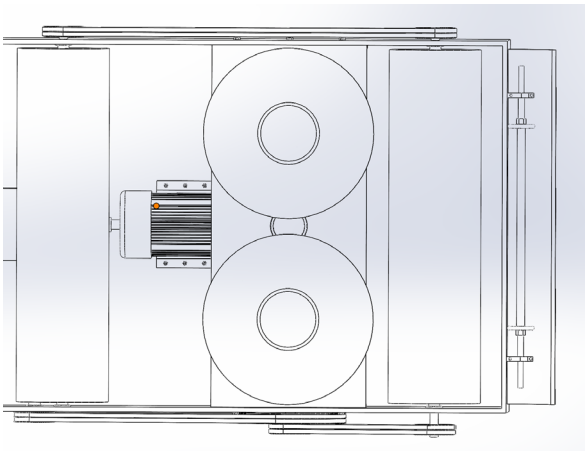

Fig. 4. Cleaning mechanism

This article uses a rolling brush as a cleaning mechanism to complete the cleaning of sediment and dust, as shown in Fig. 5. The connecting piece is fixedly connected to the walking mechanism support frame through bolts. The dust shield is installed above the rolling brush, with one end fixed to the connecting piece and the other end connected to the walking support part, which can prevent secondary pollution of the photovoltaic module caused by dust during the cleaning process. At the same time, the cleaning mechanism includes a sand or dust

recovery device, which is used to store dirt. The walking support part is equipped with two auxiliary wheels. The auxiliary wheels come into contact with the lower end of the aluminum alloy frame of the photovoltaic module, playing an auxiliary support role. Together with the walking mechanism, they drive the cleaning mechanism to move on the surface of the photovoltaic module. The cleaning drive motor is fixedly connected to the walking support part through the motor mounting plate. One end of the roller brush shaft is fixedly connected to the motor shaft, and the other end is fixedly matched with the inner ring of the diamond bearing seat on the connecting piece. The roller brush contacts the surface of the photovoltaic module with a certain pressure. When the robot walking mechanism drives the cleaning mechanism to move, the cleaning drive motor rotates the roller brush itself, achieving surface cleaning of the photovoltaic module.

In summary, this chapter has completed the main structural design of the robot, and then provided a more detailed design process for the main structure, namely the cleaning structure. The robot structure serves as the structural foundation for the robot to achieve photovoltaic panel cleaning function, laying the foundation for further control system design and path planning.

4 Control System Design and Path Planning Methods

This article first models and designs a motor control system for DC motors. Then, it compares and analyzes the advantages and disadvantages of several types of dual motor synchronous control and control strategies, and proposes a fuzzy rule-based synchronous control strategy, namely the PID (Proportional-Integral-Derivative control) control strategy. In the control strategy, proportion, integral, and differential are three important parameters that determine the control effect of the control strategy. In order to obtain the optimal combination of the three parameters, this article uses an improved neural network to solve the parameters. For the path planning method for robots, a typical surface structure diagram of photovoltaic panels is first designed, and then an improved ant colony algorithm is used to solve the path according to the cleaning rules [15].

4.1 PID Controller Modeling Design

The schematic diagram of the PID controller is shown in Fig. 5. The main control components include a linear combination of proportional K_p, integral K_i, and differential K_d. After forming a new control variable, the controlled object is then controlled [16].

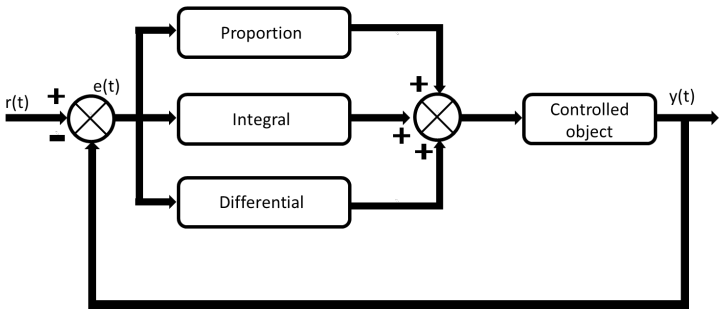

Fig. 5. PID controller schematic diagram

$r(t)$ is the input of the system, $y(t)$ is the output of the system, $e(t)$ is the deviation value of the system feedback link, K_p is the proportional coefficient, K_i is the integral coefficient, K_d is the differential coefficient, and the discretized discrete PID expression is:

$$u(k) = K_p e(k) + K_i \sum_{i=0}^{k} e(i) + K_d \left[e(k) - e(k-1) \right]. \tag{4}$$

In order to achieve a practical and reasonable PID controller, it is first necessary to establish a suitable motor model. During the operation of DC motors, there are mainly mechanical processes of motor speed changes and electromagnetic processes of electric quantity changes. In reality, they occur simultaneously. Therefore, starting from the instantaneous state of DC motor operation, the transfer function of the motor can be determined by establishing the balance equation of armature voltage and torque balance equation [17].

$$\begin{cases} u_a(t) = Ri_a(t) + L\dfrac{di_a(t)}{d_t} + C_E \cdot w(t) \\ J\dfrac{dw(t)}{dt} = C_M \cdot i_a(t) - M_{fz} \end{cases} . \tag{5}$$

R represents the equivalent resistance of the armature winding resistance; L represents the equivalent inductance of the armature winding resistance; E represents the back electromotive force during motor operation; The back electromotive force coefficient is C_E; w represents the rotor speed; M_e represents the electromagnetic torque of the motor, with a torque coefficient of C_M; M_{fz} indicates the load torque; J represents the equivalent rotational inertia, and $i_a(t)$ represents the phase current.

The transfer function diagram of a DC motor is shown in Fig. 6.

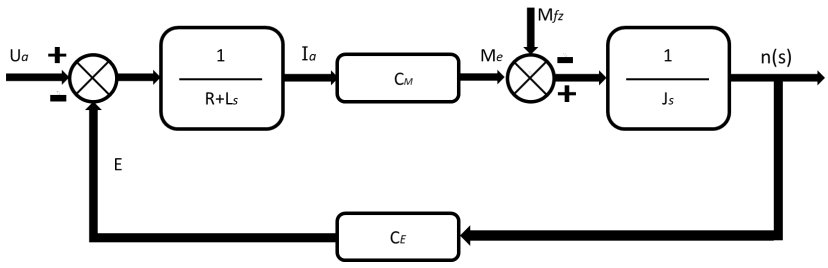

Fig. 6. Block diagram of transfer function for DC motors

In order to better regulate the controller, a neural network is added to the neural network PID controller, which determines the role of the PID controller hyperparameters (K_p, K_i, K_d). The network structure is shown in Fig. 7.

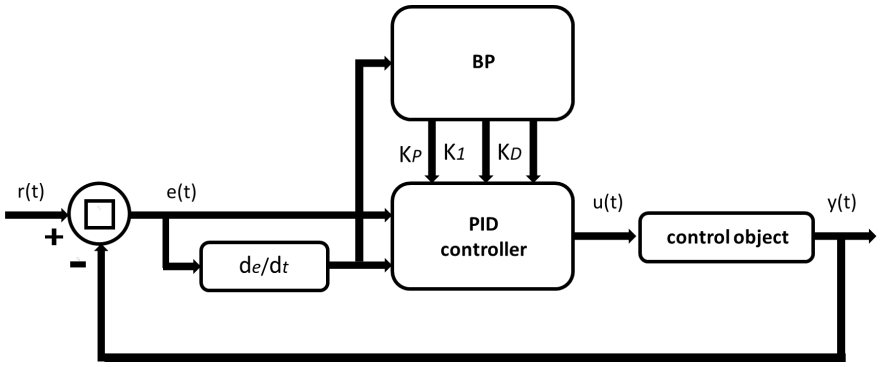

Fig. 7. Improved neural network controller

The neural network PID controller mainly utilizes the good learning ability and non-linear processing ability of the neural network to train samples/datasets, change the three main parameters K_p, K_i, K_d in traditional PID controllers, and achieve effective control of complex systems. The BP neural network adjusts the PID control pa-

rameters online to form the BP-PID control algorithm [18]. The algorithm flowchart is shown in Fig. 8.

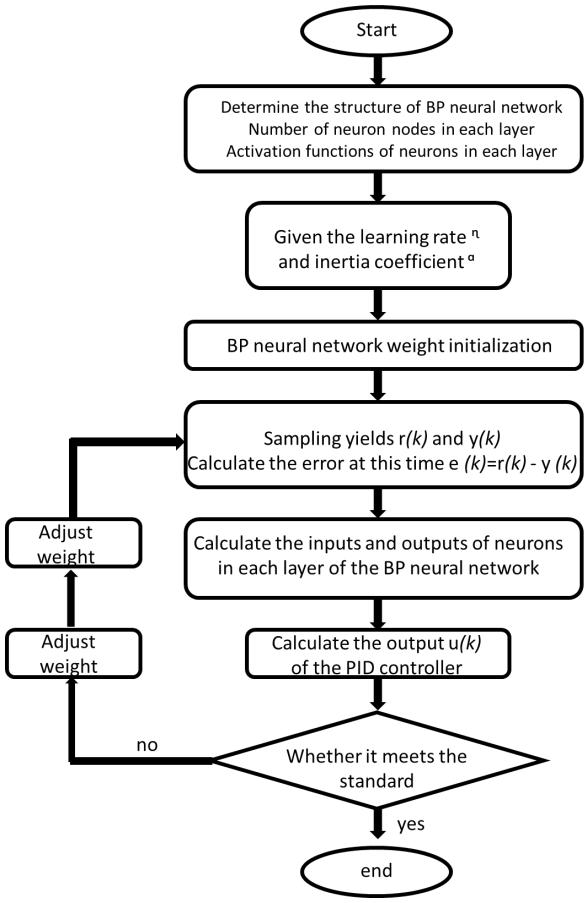

Fig. 8. Algorithm flow chart

Therefore, based on the motor parameters in Table 1, a PID motor control system was built in Matlab/Simulink for simulation, as shown in Fig. 9. Firstly, set the initial values of the three parameters, then set the constraints of the BP neural network, and then use the BP neural network to solve the three parameter values K_p, K_i, K_d in the controller. The order of parameter adjustment is proportional first, integral second, and then differential. At the same time, when adjusting, the impact of the changes in the size of the three parameter values on the system performance should be considered.

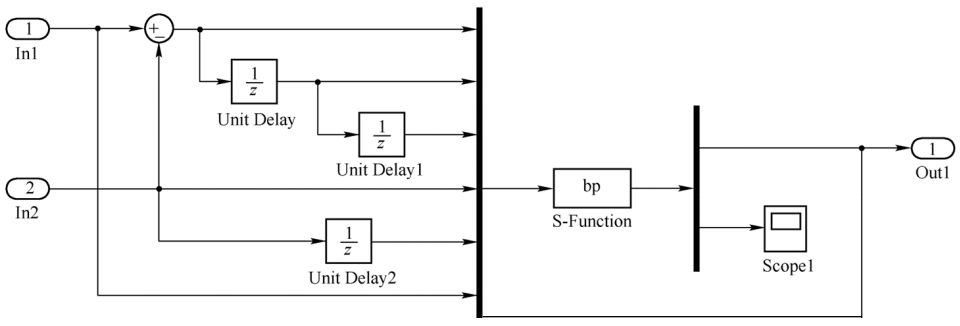

Fig. 9. Algorithm flow chart

4.2 Robot Path Planning

According to the power output requirements of solar power plants, cleaning robots need to complete the cleaning work of solar photovoltaic panels in their jurisdiction during the cleaning cycle, in order to improve the efficiency of solar energy conversion into electricity in the northwest wind and sand weather. According to the cleaning requirements, the cleaning robot travels to the designated starting point of the cleaning work for the day based on the global intelligent planning path results in the panoramic map within each working day. Then, it stops the cleaning work for the day at the end point and automatically returns to the dedicated parking rack of the cleaning robot. After analysis, this article uses the arrangement matrix of photovoltaic panels in solar power plants to provide the variation law of robot working cycle position. The schematic diagram of the law is shown in Fig. 10. This article uses an improved grid environment modeling method to construct an environment model, simulating the situation where the robot needs to clean various local areas of solar photovoltaic panels within 6 days.

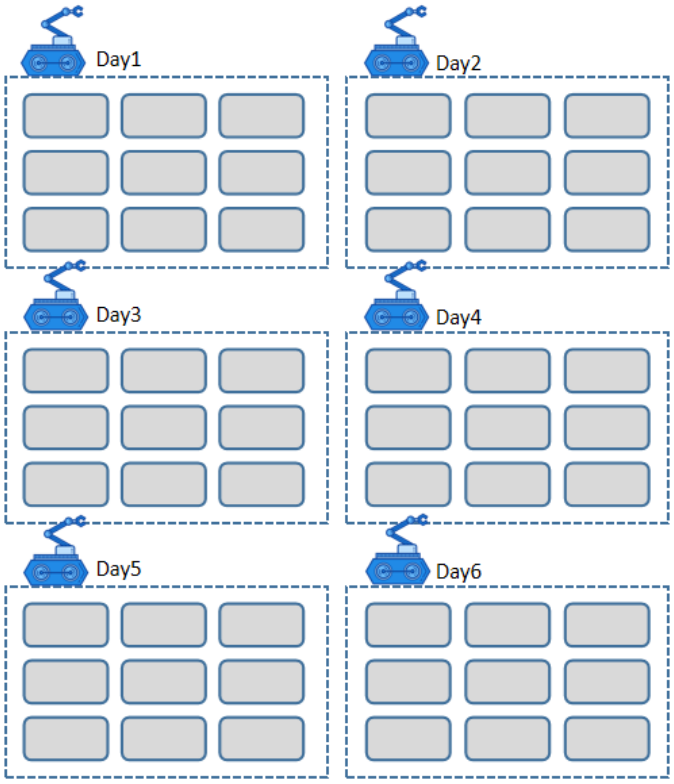

Fig. 10. Position changes during robot work cycle

This article uses ant colony algorithm to plan the robot path, where l_{ij} represents the distance $i, j = 1, 2, ..., n$ from cleaning position i to cleaning position j. The planning goal is for the cleaning robot to automatically avoid obstacles from the workstation and reach the initial cleaning position of the day. The path distance obtained from the search for the planned route is the shortest, and the path can be far away from the dense solar photovoltaic panel matrix to achieve a safer goal. The number of ants n, $i = (1, 2, ..., m)$ is the cleaning position of the cleaning robot at a certain moment, that is, the number of ants at node i. When ants perform path search:

1) When reaching the cleaning position of a robot, it is necessary to select the next node, that is, the next cleaning position, based on the probability function of hormone intensity.

2) The cleaning robot can only walk on a safe path and cannot return to the previously passed cleaning position point, unless the cleaning cycle is updated, which is controlled by a taboo table, which lists the cleaned area as a taboo point to pass through. $jinji^k$ represents the taboo list of the k -th ant, and $jinji^k(S)$ represents the S-th element in the taboo list.

3) After completing all path searches within a cleaning cycle, the ants in the algorithm leave pheromones at each cleaning location they visit. At the initial moment, the pheromone of each path is the initial value C, set to 0.

One of the ants determines the direction of the next node based on the residual amount of information on each path during the motion search path. This represents the probability of the ant transferring from cleaning position i to the next cleaning position j at this moment, which is given by the following equation.

$$p_{ij}^{k}(t)=\begin{cases}\dfrac{\left[\tau_{ij}(t)\right]^{\alpha}\left[\eta_{ik}(t)\right]^{\beta}}{\sum\left[\tau_{is}(t)\right]^{\alpha}\left[\eta_{is}(t)\right]^{\beta}} \\ j\in yunxu^{k}, s\subset yunxu^{k} \\ \\ 0, other\end{cases} \tag{6}$$

Among them, $yunxu^{k}=\{0, 1, ..., n-1\}-jinji^{k}$ represents that ant k selects the next cleaning position allowed to pass through from the taboo table. Unlike real ant colonies in nature, the artificial intelligence ant colony algorithm has memory and storage functions after each path cycle. $jinji^{k}$ is used to record all the cleaning positions that ant k has experienced before this moment, and updates and adjusts the $jinji^{k}$ set without passing through any cleaning position. τ represents the heuristic degree of the pheromones left by each ant after passing through a route, represented by a mathematical model. Generally, $\tau = 1/ l_{ij}$ is taken, and l_{ij} represents the distance between cleaning position i and cleaning position j [19]. After n moments, the ant completes one cycle, and the amount of information on each path needs to be adjusted according to the following formula:

$$\tau_{ij}(t+h)=(1-\varsigma)\tau_{ij}+\varsigma\tau_{0}. \tag{7}$$

The search steps of ant colony algorithm are as follows:

Step 1: At time $t = 0$, the expected $E = 0$ of the membership cloud is determined by the normal distribution bandwidth $b = N_{max}/ 3$, where N_{max} is the maximum iteration number of the ant colony algorithm. The maximum variance σ_{max}, maximum pheromone intensity Q_{max}, and maximum pheromone volatilization coefficient ρ_{max} are set.

The parameters that need to be adaptively adjusted in ant colony algorithm are constrained and adjusted through a membership cloud model with normal distribution rules, and the heuristic function parameters and volatility function parameters of ant colony algorithm are generated using a membership cloud generator. For pheromone intensity Q, extract it from the left half of the normal distribution surface of the membership cloud model, and for pheromone volatility function p, extract it from the right half of the normal distribution surface of the membership cloud model [20]. The search steps of ant colony algorithm are as follows:

Step 2: $t = t +1$;

Step 3: $x = t - N_{max}$, use the U condition membership cloud to generate cloud droplets that match the numerical features;

Step 4: $Q(t) = Q_{max}\,\mu_1$; $\rho(t) = \rho_{max}\mu_2$;

Step 5: If the optimal solution does not improve after several generations, return to Step 2

In summary, after each iteration of the algorithm, the optimal planned route in this iteration is found and saved. After analysis, the ant with the shortest path updates the pheromone concentration, and the updated pheromone can take effect before entering the next search cycle [21].

5 Simulation of Robot Structure and Path Planning

According to the structural design in Chapter 3, the cleaning shaft of the robot is fixed at both ends. During the working process, it bears a large torsional force, as well as its own gravity and the support force of the bearing seat. By analyzing its dynamic and static characteristics, the structural design of the cleaning shaft can be optimized, making it have good dynamic response characteristics during the working process and improving the motion stability of the entire cleaning robot. Establish a three-dimensional model of the cleaning shaft in ABAQUS,

with the weight of the rotor acting as a non load on the main shaft. After simplifying the model of the entire shaft, it is treated as a plane beam. The three-dimensional model is shown in Fig. 11.

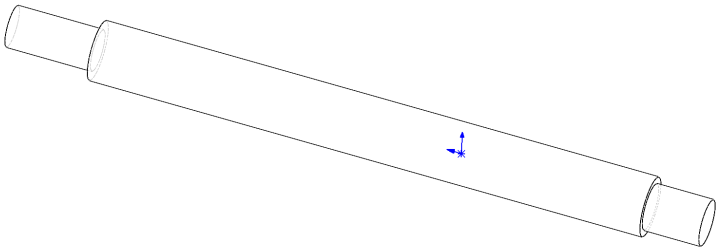

Fig. 11. 3D model of axis

The material is set to aviation aluminum alloy, with a density of $2.75\times10^{-9}\,g/mm^3$, an elastic modulus of $7.05\times10^5\,N\bullet mm^{-2}$, and a Poisson's ratio of 0.33. Through ABAQUS simulation analysis and calculation, the maximum offset of the axis is 1.3*mm*, and the finite element analysis results are shown in Fig. 12.

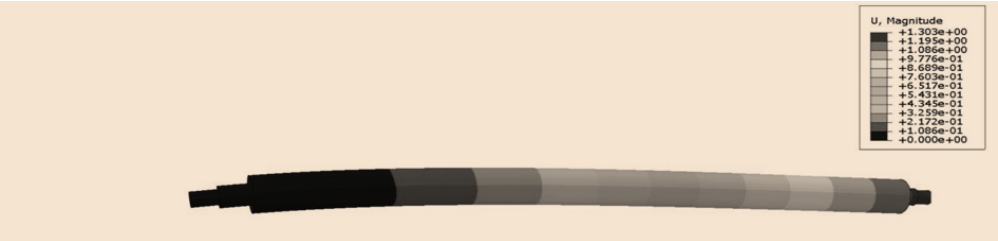

Fig. 12. Finite element analysis results

Similarly, simulation results under other working conditions can be obtained. The natural frequency of the cleaning shaft is increasing, and the first critical speed is much higher than the rated working speed of 220rpm. Therefore, the design of the cleaning shaft meets the design requirements and avoids resonance phenomena.

The computer is installed on the PC side of the Windows 10 system, with an Intel Core i7-8750H processor, Nvidia's 1080Ti GPU, and 8GB of CPU memory. The simulation environment parameters for path planning are shown in Table 2.

Table 2. Ant colony algorithm parameter settings

Parameter	Parameter values
Ant number	50
Maximum pheromone value	10
Pheromone minimum value	6
Pheromone factor	1.0
Pheromone decay constant	0.9
Pheromone intensity factor	1

Test the algorithm for robot trajectory tracking at the rooftop power station, collect the coordinates of the area boundary in advance according to the method in the first section, and then generate the vertices of each straight line trajectory. Based on the order of the vertices, determine the order of the robot's cleaning trajectory and the direction of each straight line trajectory. The robot cleans horizontally at a distance of approximately 8*m* and

moves longitudinally at a distance of 0.6*m*. Compare the actual running trajectory with the calculated trajectory. The comparison results are shown in Fig. 13.

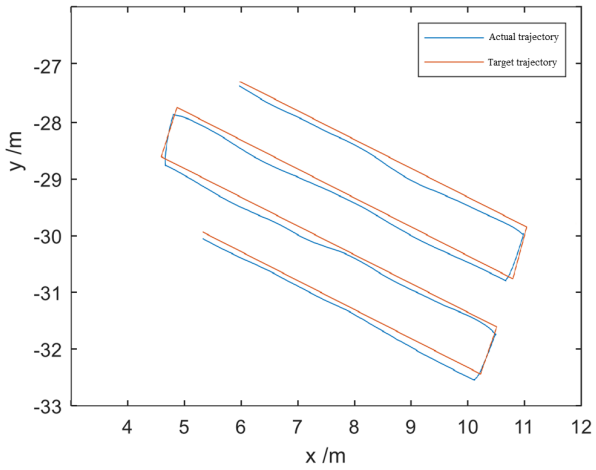

Fig. 13. Finite element analysis results

The actual running trajectory of a robot has two characteristics: firstly, the robot will always maintain a distance deviation from the target trajectory without further adjusting the running trajectory; The second is that the robot generates new errors at each turning point, which is a sudden change in distance deviation.

In summary, based on the traditional ant colony algorithm, this article improves the traditional grid modeling method by establishing important information such as displacement and danger, and adding a lightning hazard coefficient, so that the cleaning robot can more intelligently avoid dense solar photovoltaic panel arrays. This method is simple and feasible, providing a good solution for solving the path planning problem of large-scale solar power plants using robots to complete cleaning operations in complex terrain environments in western China, and has certain practical value.

6 Conclusion

This article focuses on how to achieve efficient cleaning of photovoltaic panel surfaces, and designs and analyzes the design and path planning of photovoltaic panel robots. Firstly, the construction environment of photovoltaic power stations was analyzed, including the arid and rainless northwest region, urban areas, and rural rooftops. Based on the working environment of the robot, this study designed a mobile photovoltaic cleaning robot with efficient cleaning performance to effectively clean the surface dirt of photovoltaic panels. At the same time, research was conducted on the control system of the cleaning robot based on PID control strategy. For the solution of control strategy parameters, ant colony algorithm was used in this paper, and the trajectory planning of the cleaning path of the robot on the photovoltaic panel was finally achieved, which improved the cleaning efficiency of the robot. At the end of the article, simulation modeling and analysis were conducted on the transmission shaft of the robot's cleaning mechanism, and its fatigue strength was verified. In the functional design phase, it should be considered to design the robot as a lithium-ion battery powered mode, and install an automatic charging device near the parking rack. The power of the automatic charging device comes from the photovoltaic power generation system, aiming to achieve a fully automatic and unmanned working mode for the photovoltaic cleaning robot.

The current cleaning robots are generally divided into water-based and waterless cleaning robots, as well as water-based and waterless switching robots. However, water-based robots carry water storage bags, which increases the weight of the robot and reduces the working time. Therefore, in the future, more in-depth research can be conducted on cleaning mechanisms to propose more effective cleaning methods for the types of stains on photovoltaic panels, so that the operation of robots is not limited by cleaning mechanisms. In addition, this

article did not study the scheduling system of cleaning robots. In large photovoltaic panel arrays, relying solely on a single robot to complete cleaning work would result in low work efficiency. When multiple cleaning robots collaborate to complete the cleaning work of photovoltaic panels in photovoltaic power plants, it is necessary to schedule multiple robots reasonably to avoid collisions between subsequent robots. Therefore, path planning methods based on multi robot collaborative scheduling will be further research directions in this article.

Considering the cost of manual management and maintenance, the robot designed in this article should add IoT functionality, which means that the operation status of the robot, the cleaning status of the robot, and the wear and tear of various components of the robot can be remotely transmitted in real time. The backend management personnel can manage all robots and schedule their operation and maintenance through the control center.

7 Acknowledgement

Bingtuan Xingxin Vocational and Technical College 2024 Scientific Research Project: Research on the Characteristics and Removal Technology of Micro scale Dust Particles in Photovoltaic Cells. Project No. YJZDKT202314.

Tiemenguan City 2024 Science and Technology Plan Project: Theoretical study on adhesion and removal of dust particles on the surface of photovoltaic panels. Project No. 2024RC0303.

References

[1] B. Huang, W. Zhao, L.-D. Liao, M. Xiao, J.-L. Huang, P.-L. Xie, Analysis on Regional Difference of the Whole PV Industry Chain from the Perspective of Policy, Southern Energy Construction 11(2)(2024) 179-188.

[2] Z. Qu, S.-C. Yang, J.-H. Xiao, Current situation and potential of photovoltaic power plant construction in northwestern China under the background of carbon peaking and carbon neutrality, Journal of Arid Land Resources and Environment 38(2)(2024) 20-26.

[3] S.-Q. Wang, K. Wei, J.-H. Zhang, X.-S. Li, Investigation on the Dust Accumulation Characteristics and Cleaning Effect of PV Power Stations in Qinghai Province, Electric Power Survey & Design (30)(2024) 18-22.

[4] L. Han, Static Analysis for Walking Mechanism of the Solar PV Module Cleaning Robot, Mechanical Management and Development 39(4)(2024) 28-30.

[5] A.-M. Jiang, Y. Zhang, Z. Tong, S. Gao, Research on intelligent robot design based on component cleaning model, Adhesion 50(7)(2023) 137-140.

[6] Y.-C. Wu, Influence of Dust Accumulation on Power Generation of PV Power Station and Analysis of Cleaning Methods, Solar Energy (9)(2021) 47-51.

[7] M.-U. Khan, M. Abbas, M.-M. Khan, A. Kousar, M. Alam, Y. Massoud, S.H.M. Jafri, Modeling and design of low-cost automatic self cleaning mechanism for standalone micro PV systems, Sustainable Energy Technologies and Assessments 43(2021) 100922.1-100922.10.

[8] S.-J. Xu, J. Jiao, M. Li, H.-L. Li, X.-J. Yang, X.-W. Liu, P.-P. Guo, Z.-R. Ma, Path planning and motion control method for sick and dead animal transport robots integrating improved A* algorithm and fuzzy PID, Smart Agriculture 5(4) (2023) 127-136.

[9] L. Peng, D.-W. Tang, G. Chen, Analysis of Automatic Driving Error of Robot Based on Fractional-order PID, Mechanical & Electrical Engineering Technology 52(2)(2023) 134-138.

[10] Z.-F. Liu, L.-H. Zhang, N.-X. Wei, X.-F. Kuang, Research on gridding and path planning of environmental map, Ship Science and Technology 52(2)(2021) 141-145.

[11] K.-Y. Wang, Z. Shi, Z.-C. Yang, Y.-H. Yang, S.-S. Wang, Path Planning for Mobile Robot Using Improved Reinforcement Learning Algorithm, Computer Engineering and Applications 57(18)(2021) 270-274.

[12] B. Guo, Y. Liu, Y. Ye, X.-S. Li, J.-A. Yang, Research on Dust Accumulation Characteristics and Cleaning Methods of Photovoltaic Power Stations in Gansu Province, Water Power 49(10)(2023) 109-115.

[13] R.-X. Li, R.-X. Yang, X. Wu, Y.-Y. Wu, Design and Optimization of Photovoltaic Energy Supplement Project for Net Zero Energy Consumption Demonstration Building, Construction Science and Technology (21)(2021) 78-82.

[14] J. Zhang, Y. Ying, P. Song, Z.-Q. Chen, S.-A. Wang, M.-Y. Gao, Z.-K. Dong, A study of memristive neural network based photovoltaic panel cleaning robot PID controller, Renewable Energy Resources 39(1)(2021) 37-44.

[15] H.-S. Liu, H.-B. Liu, Speed Adaptive Control Strategy of Permanent Magnet Synchronous Motor Based on RBF Neural Network, Chinese Journal of Electron Devices 46(6)(2023) 1552-1560.

[16] L. Shi, Z.-D. Xiao, Z.-N. Wang, D.-J. Wang, S.-J. Yang, Research on the Ship Model Heading Control Based on Fuzzy PID, Microcomputer Applications 38(12)(2022) 89-92.

[17] W.-J. Liu, X.-Z. Hu, Research on stepper motor control algorithm of emergency rescue robot based on BP-PID, Journal

of North China Institute of Science and Technology 21(2)(2024) 44-48.
[18] P. Qian, C.-D. Gu, X.-F. Xian, Y. Liu, Path planning of underwater robot based on improved ant colony algorithm, Manufacturing Automation 44(12)(2022) 181-184+208.
[19] Y.-J. Zeng, B. Chen, R. Qu, M. Li, Research on path planning of mobile robot based on improved ant colony algorithm, Modern Manufacturing Engineering (10)(2023) 57-63+119.
[20] C.-M. Li, J. Gong, W.-C. Niu, C. Wang, Combinatorial Optimization of Spray Painting Robot Tool Trajectory Based on Improved Membership Cloud Models Ant Colony Algorithm, Journal of Shanghai Jiaotong University 49(3)(2015) 387-391.
[21] L. An, C.-G. Zhang, J.-H. Liu, J.-R. Liu, Y.-B. Yang, Optimized Design of Permanent Magnet Adsorption Device for Wall−Climbing Robot based on DOE, Mechanical Research & Application 36(6)(2023) 59-62+68.